DEPRESSING THE EFFECTS OF SPECKLE SIGNALS IN SAR SATELLITE IMAGES USING ADDITIVE AND MULTIPLICATIVE MODELS

Yishuo Huang[1], Yu-Chen Huang[2] and Sang-Yuh Lin[1]

[1] Department of Construction Engineering, Chaoyang University of Technology, 168, Jifeng E. Rd., Wufeng District, Taichung, 41349, Taiwan.
E-mail:yishuo@cyut.edu.tw, sylin@cyut.edu.tw.

[2]Ph.D Candidate, Department of Civil Engineering, National Chung-Hsing University, 250 Kuo-Kuang Rd., Taichung, 402, Taiwan
E-mail: yuchen 131@gmail.com

KEYWORDS: SAR images, speckle signals, level set

ABSTRACT: Synthetic aperture radar (SAR) provides a remote sensing technique to explore the ground truth in all weather conditions. However, interpretation of SAR images is difficult because of the effects of speckle signals. In this paper, we decompose a given SAR image into two parts: low frequency and high frequency. For the low frequency part, the piecewise-constant approximation implemented with a level set approach is used with modeling of sharp edges. The high frequency part, capturing global intensity inhomogeneities, is illustrated by minimizing the energy defined in the model proposed by Mumford and Shah. Based on the fact that the segmented regions are homogeneous and presented as regional constants, the energy defined by the segmented regions and their corresponding regional boundaries is minimized, such that the relationships between the defined energy and the implicit functions can be transformed into the relationships between the implicit functions and time. By implementing the proposed algorithm in terms of finite differences, this method offers an efficient and stable approach for determining a numerical solution. By increasing iterations and preselected level values, the implicit functions evolve close to the regional boundaries based on the energy minimization. In this paper, the additive and multiplicative models are used to evaluate their performance in depressing the effects of speckle signals appearing in a given SAR image.

1. INTRODUCTION

Synthetic aperture radar (SAR) provides a remote sensing technique to explore the ground truth in all weather conditions. Interpreting SAR images plays an important part in analyzing the Earth’s surface characteristics in the imaged areas. Segmenting SAR images into a series of homogeneous sub-regions is a fundamental step in SAR image interpretation. However, the effects of speckle signals make the interpretation of SAR satellite images difficult. For SAR image interpretation, a consideration of the effects of speckle signals is necessary to develop SAR segmentation algorithms.

Removing the effects of speckle signals is a critical step in SAR image segmentation. In general, there are two ways to deal with the problems caused by speckle signals in currently developed SAR segmentation algorithms. One way is to use the developed filters to depress the effects of speckle signals and then apply segmentation algorithms to a given SAR image to segment the entire image. The filters developed for removing the effects of speckle signals are based on averaging pixels within a homogeneous region (Lee, 2009), or applying an improved edge detector to filter out the speckle signals (Germain, 2000). These developed filters depend heavily on the architecture of the analyzing windows (Chan, 2000). With the filtered SAR images, several approaches employing different neural network algorithms have been proposed to segment the given SAR images. Karvonen applied pulse-coupled networks to segment the Baltic Sea ice SAR images to study the properties of sea ice (Karvonen, 2004). Davison has employed the multilayer perceptron network to classify ERS-1 SAR imagery for crop discrimination (Davison, 1994). These researchers have successfully implemented different neural network algorithms to classify a given SAR image into several groups to study the information hidden in the classified results. The accuracy of the classified results is heavily dependent upon the properties of the selected training data sets and the structures of the developed filters. However, the filtered SAR images usually have problems related to the bias in the filtered data, blurring and suppressing highly reflective points (Lee, 2009). Another approach based on the assumption that the segmented regions can be approximated by those segmented regional averages has been recently proposed (Osher, 2002).

Segmentation algorithms implemented with the curve evolution and level sets approaches have been successfully applied to optical images and thermal infrared images (Osher, 2002; Huang, 2010; Kass, 1988). The idea of an evolving curve can be traced back to the late 1980s. The concept of an evolving curve is that an initial curve will automatically move to the regional boundaries according to the principle of minimum energy. In 1988, Kass and Witkin proposed the snake theory, where extracting regional boundaries with the iteration approach is based on minimizing the energy contained in the image (Chesnaud, 2001). The classical snake algorithm was implemented and applied to segment SAR images (Ayed, 2005). There are existing limitations for the snake algorithm: the topology of the evolving curves will be affected during evolution, and the procedures of segmentation depend on parameterization (Yang, 2009). Although Ayed *et al.* proposed segmenting the entire SAR image into a number of *N* sub-regions by applying active curve evolutions through level sets, a new approach has been developed to handle the topological changes of the evolving curves (Ayed, 2005; Yang, 2009; Chung, 2009).

In this paper, the additive and multiplicative models for a given SAR image are evaluated. In the field of image processing, the issue of how to extract meaningful information from a given image can be formulated as an inverse problem: given an image *f*, find an approximation *u* such that *u* is close to *f*. Often, *u* is an image containing homogeneous sub-regions and boundaries. Most image models assume that there is an additive relation between *f* and *u*: $f = u + v$, where *v* is texture information. In general, the component *v* is ignored. Similarly, the multiplicative model is especially suited for SAR image interpretation: $f = uv$. However, the component *v* is important in some cases, if it is employed to represent texture information. Texture can be defined as a repeated pattern of small-scale details (Vese and Osher, 2003). Similarly, the noise is a random pattern of small-scale details. Both types of patterns (noise and texture) can be modeled by oscillatory functions taking both positive and negative values, with a mean of zero (Meyer, 2002).

This paper employs the multilayer level set approach to decompose a given SAR image into *u* and *v*, according to the additive and multiplicative models. The remainder of this paper is organized as follows. In the next section, the minimal partition problem proposed by Mumford and Shah is introduced (Mumford and Shah, 1988). In Section III, a short review of the additive model and multiplicative models is given and the multilayer level set approach is derived for SAR images. Section IV illustrates the processed results by employing the multilayer level set approach on real SAR images. Finally, some conclusions and related discussions are provided in Section V.

2. MATHEMATICAL MODEL OF MUMFORD AND SHAH

The goal of image segmentation is to partition the image into a series of sub-regions such that each sub-region is homogeneous. Mumford and Shah modeled the segmentation problem in computer vision. Le and Vese have proved that with few modifications, the Mumford and Shah Models can effectively depress the additive and multiplicative noise in the segmentation problems (Le and Vese, 2007). The definition is given as follows: given an image I_0, let $\mathrm{I}_0 : \Omega \to \mathrm{R}$ be a given bounded image function and, from the point of view of approximation theory, find a decomposition $\Omega = \bigcup_i \Omega_i \bigcup \mathrm{C}$ and an optimal piecewise-smooth approximation **I** of I_0, such that **I** varies smoothly within each Ω_i and **I** varies discontinuously and rapidly across the boundaries **C** between different sub-regions [17]. To solve this problem, Mumford and Shah proposed minimizing the energy function. Its mathematical model is given as follows:

$$E(\mathrm{I},\mathrm{C}) = \int_\Omega (\mathrm{I}_0 - \mathrm{I})^2 dxdy + \mu \int_{\Omega \setminus C} |\nabla \mathrm{I}|^2 dxdy + \nu |C| , \tag{1}$$

where $|\mathrm{C}|$ is the total length of the arcs making up **C**, and μ and ν are fixed parameters to weight the different terms shown in (1). In (1), the first term represents the difference between the approximation **I** and the original image I_0, the second term ensures that **I** is varying smoothly in each Ω_i, and the last term controls the length of the boundaries, so that they are as short as possible (Goodman, 1975). Let **I** be a piecewise-constant function, i.e., $\mathrm{I} = c_i$ in each Ω_i. Then, (1) can be simply represented as:

$$E(\mathrm{I},\mathrm{C}) = \sum_i \int_{\Omega_i} (\mathrm{I}_0 - \mathrm{I})^2 dxdy + \nu |C| . \tag{2}$$

Usually, the constant c_i in Ω_i can be represented as the average value in Ω_i. The mathematical proofs for the existence and regularity of minimizing (2) can be found in the work of Goodman (Goodman, 1975). The algorithm proposed by Mumford and Shah apparently works effectively on SAR images. The constant c_i is defined as follows:

$$c_i = \int_{\Omega_i} \mathrm{I}(x) dx \Big/ \int_{\Omega_i} dx . \tag{3}$$

3. ADDITIVE AND MULTIPLICATIVE MODELS

Segmenting SAR images can usually be done by applying clustering algorithms on the filtered images. Otherwise, curve evolution based on the model developed by Mumford and Shah is used to segment those unfiltered SAR images. In this section, the additive and multiplicative models based on the multilayer level set approach are given separately. The multilayer level set approach is a type of unsupervised classification method, and employs curve evolution based on the model developed by Mumford and Shah (Mumford and Shah, 1988).

3.1 Background of Additive and Multiplicative Models

Meyer has proven that the additive model developed by Rudin, Osher and Fatemi will remove the texture information if the tuning parameter λ is small enough (Meyer, 2002). Meyer proposed the use of a space of functions to define the texture as:

$$v(x,y) = \partial_x g_1(x,y) + \partial_y g_x(x,y), \tag{4}$$

where g_1 and $g_2 \in L^\infty(R^2)$. Vese and Osher have proposed an additive model by introducing (4), and the model can be shown as follows (Vese and Osher, 2003):

$$F(u,g_1,g_2) = \int|\nabla u| + \lambda\int\left|f - u - \partial_x g_1 - \partial_y g_2\right|^2 dxdy + \mu\int\sqrt{g_1^2 + g_2^2}dxdy\,. \tag{5}$$

By minimizing the defined energy model in (5) with respect to u, g_1, and g_2, the Euler-Lagrange equations are illustrated as follows:

$$u = u_0 - \partial_x g_1 - \partial_y g_2 + \frac{1}{2\lambda}div\left(\frac{\nabla u}{|\nabla u|}\right), \tag{6}$$

$$\frac{g_1}{\sqrt{g_1^2 + g_2^2}} = 2\lambda\left[\frac{\partial}{\partial x}(u - u_0) + \partial_{xx}^2 g_1 + \partial_{xy}^2 g_2\right], \text{ and} \tag{7}$$

$$\frac{g_2}{\sqrt{g_1^2 + g_2^2}} = 2\lambda\left[\frac{\partial}{\partial x}(u - u_0) + \partial_{xy}^2 g_1 + \partial_{yy}^2 g_2\right]. \tag{8}$$

Using the finite difference approach to find the solutions of (13), (14) and (15), the numerical results are illustrated in Fig. 1 by employing parameters $\lambda = 0.1$ and $\mu = 100$ in 100 iterations.

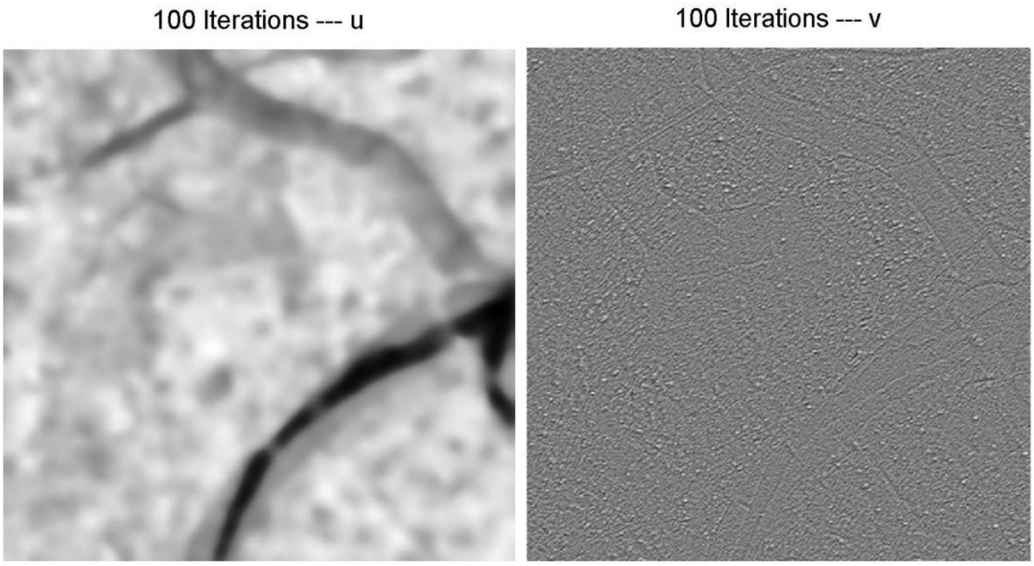

Fig. 1. The numerical result using the additive model developed by Vese and Osher, with $\lambda = 0.1$, $\mu = 100$, and 100 iterations.

Meanwhile, the multiplicative model is suitable for depressing the effects of speckle signals (Lee, 1980). Rudin proposed a multiplicative model ($u_0 = uv$) based on two constraints (Rudin, 2003):

$$\int udxdy = \int u_0 dxdy \text{ and} \tag{9}$$

$$\int(u - u_0)^2 dxdy = \sigma^2, \tag{10}$$

such that the model is defined as:

$$F(u) = \int|\nabla u|\,. \tag{11}$$

With two constraints and by minimizing (11), the Euler-Lagrange equation is shown as follows:

$$\frac{\partial u}{\partial t} = \frac{\partial}{\partial x}\left(\frac{u_x}{\sqrt{u_x^2 + u_y^2}}\right) + \frac{\partial}{\partial y}\left(\frac{u_y}{\sqrt{u_x^2 + u_y^2}}\right) - \lambda\left(\frac{u_0}{u^2}\right)\left(\frac{u_0}{u} - 1\right) - \mu\left(\frac{u_0}{u}\right). \tag{12}$$

3.2 Additive and Multiplicative Models Based on the Multilayer Level Set Approach

In the multilayer approach, let I_0 be an SAR image and the two level set functions partition a given image into sub-regions with distinct levels $\{l_1 < l_2 < \cdots < l_m\}$ and $\{k_1 < k_2 < \cdots < k_n\}$ for the level set functions ϕ_1 and ϕ_2, respectively. The relationships between the sub-regions in the approximation and the functions ϕ_1 and ϕ_2 are defined as:

$$\Omega_{ij} = \{x \in \Omega : l_i \le \phi_1(x) \le l_{i+1}, k_j \le \phi_2(x) \le k_{j+1}\}.$$

Extending (2), the energy function for the additive model is defined as:

$$\begin{aligned} E(c,\phi) = & \sum_{i,j=1}^{m-1,n-1} \int_\Omega \left|\log \mathrm{I}_0 - c_{i,j} - v\right|^2 \chi_1 dx + \sum_{i=1}^{m-1} \int_\Omega \left|\log \mathrm{I}_0 - c_{\mathrm{i},0} - v\right|^2 \chi_2 dx + \\ & \sum_{i=1}^{m-1} \int_\Omega \left|\log \mathrm{I}_0 - c_{\mathrm{i,n}} - v\right|^2 \chi_3 dx + \sum_{j=1}^{n-1} \int_\Omega \left|\log \mathrm{I}_0 - c_{0,\mathrm{j}} - v\right|^2 \chi_4 dx + \\ & \sum_{j=1}^{n-1} \int_\Omega \left|\log \mathrm{I}_0 - c_{\mathrm{m,j}} - v\right|^2 \chi_5 dx + \int_\Omega \left|\log \mathrm{I}_0 - c_{0,0} - v\right|^2 \chi_6 dx + \\ & \int_\Omega \left|\log \mathrm{I}_0 - c_{0,\mathrm{n}} - v\right|^2 \chi_7 dx + \int_\Omega \left|\log \mathrm{I}_0 - c_{\mathrm{m},0} - v\right|^2 \chi_8 dx + \int_\Omega \left|\log \mathrm{I}_0 - c_{\mathrm{m,n}} - v\right|^2 \chi_9 dx + \\ & \mu \sum_{i=1}^{m} \int_\Omega \left|\nabla H(\phi_1 - l_i)\right| dx + \mu \sum_{j=1}^{n} \int_\Omega \left|\nabla H(\phi_2(x) - k_j)\right| dx \end{aligned} \tag{13}$$

Similarly, the energy function for the multiplicative model is defined as:

$$\begin{aligned} E(c,\phi) = & \sum_{i,j=1}^{m-1,n-1} \int_\Omega \left|\frac{\log \mathrm{I}_0}{c_{i,j} v}\right|^2 \chi_1 dx + \sum_{i=1}^{m-1} \int_\Omega \left|\frac{\log \mathrm{I}_0}{c_{\mathrm{i},0} v}\right|^2 \chi_2 dx + \sum_{i=1}^{m-1} \int_\Omega \left|\frac{\log \mathrm{I}_0}{c_{\mathrm{i,n}} v}\right|^2 \chi_3 dx + \\ & \sum_{j=1}^{n-1} \int_\Omega \left|\frac{\log \mathrm{I}_0}{c_{0,\mathrm{j}} v}\right|^2 \chi_4 dx + \sum_{j=1}^{n-1} \int_\Omega \left|\frac{\log \mathrm{I}_0}{c_{\mathrm{m,j}} v}\right|^2 \chi_5 dx + \int_\Omega \left|\frac{\log \mathrm{I}_0}{c_{0,0} v}\right|^2 \chi_6 dx + \int_\Omega \left|\frac{\log \mathrm{I}_0}{c_{0,\mathrm{n}} v}\right|^2 \chi_7 dx + \\ & \int_\Omega \left|\frac{\log \mathrm{I}_0}{c_{\mathrm{m},0} v} - -\right|^2 \chi_8 dx + \int_\Omega \left|\frac{\log \mathrm{I}_0}{c_{\mathrm{m,n}} v}\right|^2 \chi_9 dx + \mu \sum_{i=1}^{m} \int_\Omega \left|\nabla H(\phi_1 - l_i)\right| dx + \mu \sum_{j=1}^{n} \int_\Omega \left|\nabla H(\phi_2(x) - k_j)\right| dx \end{aligned} \tag{14}$$

The terms $\chi_{i, i=1,2,..,9}$ are given as follows:

$\chi_1 = H(\phi_1 - l_i)H(l_{i+1} - \phi_1)H(\phi_2 - k_j)H(k_{j+1} - \phi_2)$,

$\chi_2 = H(\phi_1 - l_i)H(l_{i+1} - \phi_1)H(k_1 - \phi_2)$,

$\chi_3 = H(\phi_1 - l_i)H(l_{i+1} - \phi_1)H(\phi_2 - k_n)$,

$\chi_4 = H(l_1 - \phi_1)H(\phi_2 - k_j)H(k_{j+1} - \phi_2)$,

$\chi_5 = H(\phi_1 - l_m)H(\phi_2 - k_j)H(k_{j+1} - \phi_2)$,

$\chi_6 = H(l_1 - \phi_1)H(k_1 - \phi_2)$,

$\chi_7 = H(l_1 - \phi_1)H(\phi_2 - k_n)$,

$\chi_8 = H(\phi_1 - l_m)H(k_1 - \phi_2)$, and

$\chi_9 = H(\phi_1 - l_m)H(\phi_2 - k_n)$.

Although the Heaviside function has a different form, this paper employs the form proposed by Vese, and is defined as (Vese, 2003):

$$H(z)_\varepsilon = \frac{1}{2}\left[1 + \frac{2}{\pi}\tan^{-1}\left(\frac{z}{\varepsilon}\right)\right], \tag{15}$$

and:

$$\delta_\varepsilon(z) = H'_\varepsilon = \frac{1}{\pi}\frac{\varepsilon}{\varepsilon^2 + z^2}, \tag{16}$$

where ε is a parameter such that the function has a different zero argument while z is located in the interval $[-\varepsilon, \varepsilon]$; otherwise, the function will be zero. The sub-regional constant, c_{ij}, is the constant specified in the sub-region Ω_{ij} such that pixel values are c_{ij} in the sub-region, and is in general defined as (Chung, 2009):

$$c_{ij} = \frac{\int_\Omega (\log \mathrm{I}_0)\chi_1 dx}{\int_\Omega \chi_1 dx}. \tag{17}$$

However, other special terms, such as $c_{i,0}$, $c_{i,n}$, $c_{0,j}$, $c_{m,j}$, $c_{0,0}$, $c_{0,n}$, $c_{m,0}$, and $c_{m,n}$, can be defined as being slightly modified (10) and their mathematical representations can be found in the work of Chung (Chung, 2009).

4. NUMERICAL RESULTS

In this paper, an ERS-2 SAR image with a resolution of 12.5 m by 12.5 m was employed to evaluate the performances of the algorithm. The SAR image was collected on March 31st, 2007, and its geographic location was in the north of Taiwan. The parameters $dt=1$, $\varepsilon=1$, and $\mu=0.015\times256\times256$ were used in this paper. To implement the level set approach, two initial level set functions were given with the forms $\phi_1^0(x,y)=\sqrt{(x-x_i)^2+(y-y_i)^2}-5$ and $\phi_2^0(x,y)=\sqrt{(x-x_i-5)^2+(y-y_i-5)^2}-5$. In Fig. 2, the processed results of the additive model shown in (13) are given. In Fig. 3, the processed results of the multiplicative model shown in (14) are given.

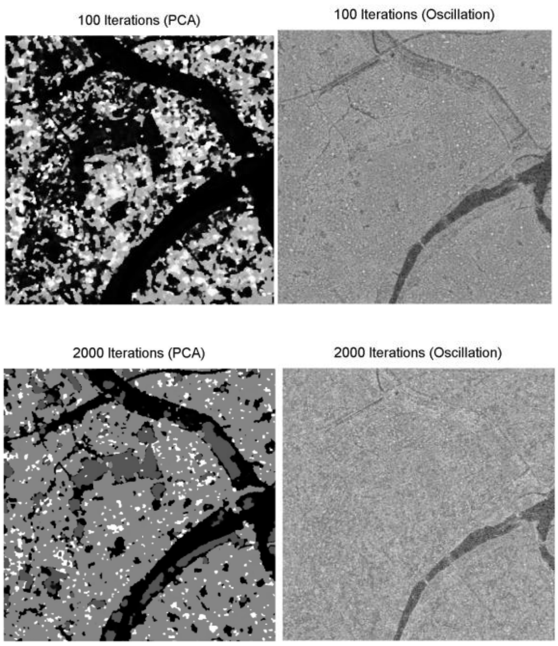

Fig. 2. The processed results of the multiplicative model shown in Eq. (13).

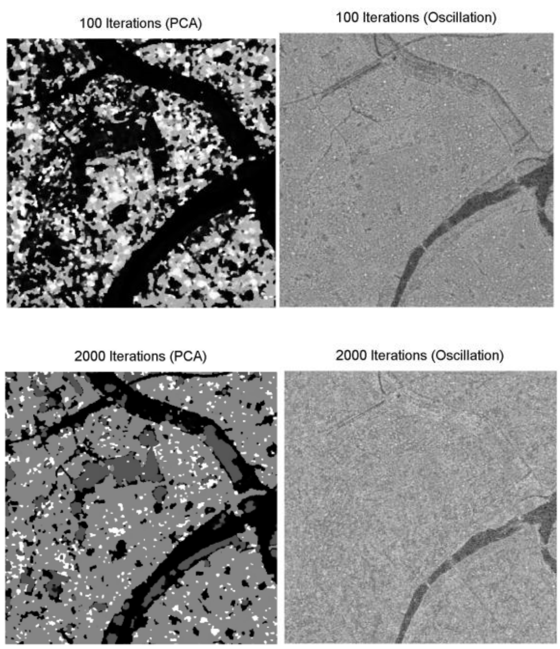

Fig. 3. The processed results of the multiplicative model shown in Eq. (14).

From the experimental results, the multilayer level set method provides a numerically stable algorithm. For a given SAR image, it requires only a few iterations to reach convergence without considering the effects of the chosen parameters. The segmented image provides a final image based on a few regional constants and the segmented regional boundaries can be built with those constants. The additive and multiplicative models are used to evaluate their performance in depressing the effects of speckle signals shown in a given SAR image. From the processed results, the proposed approach can efficiently segment any given SAR image, allowing further image interpretation to reveal the ground truth in the imaged area.

REFERENCES

Meyer, Y., 2002, Oscillating Patterns in Image Processing and Nonlinear Evolution Equations, University Lecture Series, Vol. 22, American Math. Society.

Acar, R. and Vogel, C. R., 1994, "Analysis of bounded variation penalty method of ill-posed problems, Inverse Problem 10, pp. 1217-1229.

Vese, L. and Osher, S., 2003, "Modeling Textures with Total Variation Minimization and Oscillating Patterns in Image Processing," Journal of Scientific Computing, V0. 19, N0. 1-3.

Lee, J.S., 1980, "Digital Image Enhancement and Noise Filtering by Use of Local Statistics," IEEE Trans. On PAMI, Vol. PAMI2, No.2, pp. 165-168.

Rudin, L., Lions, P. and Osher, S., 2003, "Multiplicative Denoising and Deblurring: Theory and Algorithms," Geometric Level Set Methods in Image, Vision and Graphics, edited by Stanley Osher and Nikos Paragios, Springer-Verlag New York, Inc., pp. 103-119.

Lee, J.S., Wen, J.H., Ainsworth, T.L., Chen, K.S and Chen, A.J, 2009, "Improved Sigma Filter for Speckle Filtering of SAR Imagery," *IEEE Trans.* Geoscience and Remote Sensing, Vol. 47, No. 1, pp. 202-213.

Germain, O. and Réfrégier, P., 2000, "On the Bias of the Likelihood Ratio Edge Detector for SAR Images," *IEEE Trans*. Geoscience and Remote Sensing, Vol. 38, No. 3, pp. 1455-1457, May.

Chan, T. and Vese, L., 2000, "Active Contours without Edges," *IEEE Trans.* Image Processing, Vol. 10, No.2, pp. 266-277.

Karvonen, J.A., 2004, "Baltic Sea Ice SAR Segmentation and Classification Using Modified Pulse-Coupled Neural Networks," *IEEE Trans*. Geoscience and Remote Sensing, Vol. 42, No.7, pp.1566-1574.

Osher, S. and Fedkiw, R., 2002, Level Set Methods and Dynamic Implicit Surfaces, Springer.

Huang, Y. and Wu, J.W, 2010, "Infrared Thermal Image Segmentations Employing the Multilayer Level Set Method for Non-Destructive Evaluation of Layered Structures," NDT&E International, Vol. 43, Issue 1, pp. 34-44.

Kass, M., Witkin, A. and Terzopoulos, D., 1988, "Snakes: Active contour models," Int. J. Computer Vision, Vol. 1, No. 4, pp.321-333.

Chesnaud, C. and Réfrégier, P., 2001, "Edge Location in SAR Images: Performance of the Likelihood Ratio Filter and Accuracy Improvement with an Active Contour Approach," *IEEE Trans.* Image Processing, Vol. 10, No.4, pp. 72-77.

Ayed, I.B., Mitiche, A. and Belhadj, Z., 2005, "Multiregion Level-Set Partitioning of Synthetic Aperture Radar Images," *IEEE. Trans* PAMI, Vol. 27, No. 5, pp. 793-800, May.

Yang, M.Y., 2009, "Multiregion level-set segmentation of synthetic aperture radar," 2009 IEEE International Conference Image Processing, pp. 1717-1720.

Chung, G. and Vese, L, 2009, "Image segmentation using a multilayer level-set approach," Computing and Visualization in Science, Vol. 12, No. 6, pp. 267-285.

Mumford, D. and Shah, J., 1989, "Optimal approximation by piecewise-smooth functions and associated variational problems," Communication and Pure and Applied Mathematics, 42:577-685.